Thermodynamic, Spectroscopic, and Structural Studies of Complexation of Phenol- and Pyridine-Armed Macrocyclic Ligands with Univalent Metal Ions

Xian Xin Zhang, Andrei V. Bordunov,† Xiaolan Kou, N. Kent Dalley, Reed M. Izatt,* John H. Mangum, Du Li, Jerald S. Bradshaw,* and Paul C. Hellier

Department of Chemistry and Biochemistry, Brigham Young University, Provo, Utah 84602

Received October 16, 1996[⊗]

Log *K*, ΔH, and ΔS values for interactions of a series of pyridinoazacrown ethers each bearing a phenol arm (**2**−**6**) and two macrocycles each bearing a pyridine arm (**7**, **8**) with Na^+, K^+, Tl^+, and Ag^+ have been determined in absolute methanol at 25 °C by calorimetric titration. In each case, the complex stability has the sequence $Na^+ < K^+ < Tl^+ \ll Ag^+$. The phenol-armed macrocycles exhibit selectivity of more than 4 orders of magnitude for Ag^+ over Na^+, K^+, and Tl^+. Attachment of a pendant phenol arm having various substituents to parent macrocycle **1** increases the binding abilities of the resulting ligands. Substituents on the para position of the phenol arm have an appreciable effect on cation-binding constants. Good Hammett correlations are found by plotting log *K* values vs σ_p for interactions of five phenol-armed macrocyclic ligands (**2**−**6**) with Na^+, K^+, and Tl^+. The complexation has been characterized by means of ^{1}H NMR and UV−visible spectroscopic, and X-ray crystallographic methods. The crystal data for Na^+−**3**: formula, $[Na(C_{23}H_{28.5}N_3O_5)](ClO_4)_{0.5}$; space group, $P\bar{1}$; $a = 9.400(9)$ Å, $b = 11.467(10)$ Å, $c = 12.281(11)$ Å, $\alpha = 77.22(7)°$, $\beta = 87.73(7)°$, $\gamma = 86.39(7)°$, $V = 1288(2)$ Å^3, and $Z = 2$. The study indicates that the phenol OH group of **2**−**6** is capable of forming an intramolecular hydrogen bond with the macroring nitrogen atom and that the complexation in absolute methanol generally does not deprotonate these phenols. In the crystal structure of the Na^+−**3** complex, the Na^+ is coordinated to all seven of the donor atoms of the ligand and two Na^+−**3** complexes join together to form a dimer. The dimer contains an intermolecular hydrogen bond formed between the phenol hydrogen atom of one ligand and the phenolate group of a centrosymmetrically related ligand and two $\pi-\pi$ stacking interactions between the electron-deficient pyridine ring of one molecule and the electron-rich phenol ring of the other.

Introduction

Pyridine-containing macrocycles form stable complexes with metal ions,[1−10] various ammonium cations,[10−14] and water molecules.[15] A macrocyclic ligand having a pyridine ring incorporated into its backbone usually has notably different complexation properties from its fully saturated analogues. Sherry and co-workers have recently observed that incorporation of one or two pyridine groups into tetraaza macrocycles results in a significant change in both complexation kinetics and thermodynamic properties.[5] The complexation rates of the pyridine-containing tetraaza ligands with Gd^{3+} are fast enough for potentiometric titrations to be made while the CYCLEN derivatives form complexes with Gd^{3+} too slowly for normal potentiometric titrations. Jackels and co-workers have found that incorporation of two pyridine moieties into an [18]aneN_6-type macrocycle results in an increase in binding constants for its interaction with Ca^{2+}, Zn^{2+}, and La^{3+} by up to 3 orders of magnitude over those of the parent macrocycle.[6] Thermodynamic quantities determined by Herman and co-workers indicate that the stability of the Cu^{2+} complex with a hexaaza macrocycle containing two pyridine rings is 1.5 log *K* units larger than that of the Cu^{2+} complex with the fully saturated [18]aneN_6.[7] The higher log *K* value is entirely due to an entropy effect. Because of the presence of the two pyridine groups, the macrocycle is preorganized and shows a small conformational entropic loss during the complexation.

Among seven pyridinocrown ethers of different macroring sizes (from 15-crown-5 to 33-crown-11), the 18-membered ligand was shown to have the maximum binding constants for all alkali metal cations.[4] Several pyridino macrocycles have been shown to be more effective membrane carriers for Ag^+ than the parent crown ethers.[10] Kumar, Singh, and co-workers recently synthesized a series of pyridine-containing macrocycles and studied their metal ion complexation properties.[8] They

† Present address: Division of Chemistry and Chemical Engineering 210-41, California Institute of Technology, Pasadena, CA 91125.

⊗ Abstract published in *Advance ACS Abstracts,* May 15, 1997.

(1) Izatt, R. M.; Pawlak, K.; Bradshaw, J. S.; Bruening, R. L. *Chem. Rev.* **1991**, *91*, 1721.
(2) Izatt, R. M.; Bradshaw, J. S.; Nielsen, S. A.; Lamb, J. D.; Christensen, J. J.; Sen, D. *Chem. Rev.* **1985**, *85*, 271.
(3) Kaplan, L. J.; Weisman, G. R.; Cram, D. J. *J. Org. Chem*. **1979**, *44*, 2226.
(4) Grootenhuis, P. D. J.; Van Der Wal, P. D.; Reinhoudt, D. N. *Tetrahedron* **1987**, *43*, 397.
(5) Kim, W. D.; Hrncir, D. C.; Kiefer, G. E.; Sherry, A. D. *Inorg. Chem.* **1995**, *34*, 2225.
(6) Rothermel, G. L., Jr.; Miao, L.; Hill, A. L.; Jackels, S. C. *Inorg. Chem.* **1992**, *31*, 4854.
(7) Dhont, K. I.; Herman, G. G.; Fabretti, A. C.; Lippens, W.; Goeminne, A. M. *J. Chem. Soc., Dalton Trans*. **1996**, 1753.
(8) (a) Kumar, S.; Hundal, M. S.; Kaur, N.; Singh, R.; Singh, H. *Tetrahedron Lett.* **1995**, *36*, 9543. (b) Kumar, S.; Kaur, N.; Singh, H. *Tetrahedron Lett.* **1996**, *37*, 2071.
(9) Wu, G.; Jiang, W.; Lamb, J. D.; Bradshaw, J. S.; Izatt, R. M. *J. Am. Chem. Soc.* **1991**, *113*, 6538.
(10) Bradshaw, J. S.; Maas, G. E.; Lamb, J. D.; Izatt, R. M.; Christensen, J. J. *J. Am. Chem. Soc.* **1980**, *102*, 467.
(11) Izatt, R. M.; Wang, T.; Hathaway, J. K.; Zhang, X. X.; Curtis, J. C.; Bradshaw, J. S.; Zhu, C. Y. *J. Inclusion Phenom.* **1994**, *17*, 157.
(12) Izatt, R. M.; Zhu, C. Y.; Huszthy, P.; Bradshaw, J. S. In *Crown Compounds: Toward Future Applications; Cooper*, S. R., Ed.; VCH Publishers: New York, 1992; Chapter 12.
(13) Izatt, R. M.; Zhu, C. Y.; Dalley, N. K.; Curtis, J. C.; Kou, X.-L.; Bradshaw, J. S. *J. Phys. Org. Chem.* **1992**, *5*, 656.
(14) Newcomb, M.; Timko, J. M.; Walba, D. M.; Cram, D. J. *J. Am. Chem. Soc*. **1977**, *99*, 6392.
(15) Grootenhuis, P. D. J.; Uiterwijk, J. W. H. M.; Reinhoudt, D. N.; van Staveren, C. J.; Sudhölter, E. J. R.; Bos, M.; van Eerden, J.; Klooster, W. T.; Kruise, L.; Harkema, S. *J. Am. Chem. Soc.* **1986**, *108*, 780.

S0020-1669(96)01263-3 CCC: $14.00

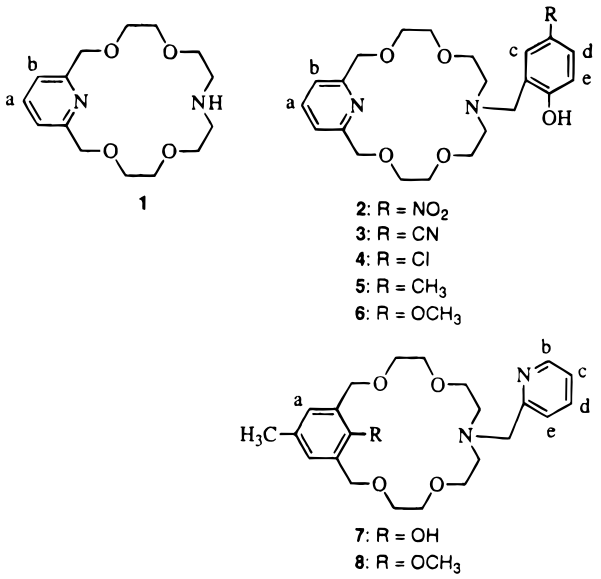

Figure 1. Structures of macrocyclic compounds.

found that several macrocycles possessing a high degree of structural organization selectively extracted Ag^+ from aqueous picrate solution into chloroform over alkali and alkaline-earth metal, Tl^+, and Pb^{2+} ions.

We recently reported the synthesis of a series of pyridinoaza-crown ethers bearing a pendant phenol arm and several macrocycles bearing a pendant pyridine arm.[16] Attachment of a phenol or pyridine arm to the crown ring provides three-dimensional coordination to guest molecules. The cooperative binding of the macroring and side arm(s) with a guest molecule has been observed.[17−19] The preliminary results reported in our previous paper[16] show that the phenol-substituted pyridino-18-crown-6 ligands (Figure 1) form stable complexes with Na^+, K^+, and Ag^+ (Table 3). In this paper, we report a systematic study of the complexation of these phenol- and pyridine-substituted macrocyclic compounds with Na^+, K^+, Tl^+, and Ag^+. Log *K*, ΔH, and $T\Delta S$ values for these interactions in methanol (MeOH) at 25 °C were determined by a calorimetric titration procedure. The macrocyclic compounds and their complexes were characterized by means of ^{1}H NMR and UV−visible spectroscopic and X-ray crystallographic methods. Substituents on the para position of the phenol arm have an appreciable effect on cation-binding constants, and good Hammett correlations are found by plotting log *K* values vs substituent constants (σ_p).

Experimental Section

Materials. Compounds **1**−**8** (see Figure 1) were synthesized as reported.[16] The purities of these macrocyclic compounds were found to be 99.0−99.9% by ^{1}H NMR spectroscopy and thermometric titration analyses. The purities of the metal ion salts, NaBr (J. T. Baker), $NaNO_3$ (Aldrich), KBr (Wasatch), thallium acetate CH_3CO_2Tl (Aldrich), and $AgNO_3$ (EM Science), were greater than 99.9%. The salts were used without further purification. MeOH was of HPLC grade (Fisher) and had a water content of less than 0.05%.

Determination of Thermodynamic Quantities. Log *K*, ΔH, and $T\Delta S$ values were determined in absolute MeOH at 25.0 ± 0.1°C by titration calorimetry as described earlier[20] using a Tronac Model 450 calorimeter equipped with a 20-mL reaction vessel. The metal ion solutions were titrated into the macrocyclic ligand solutions, and the titrations were carried out to a 2-fold excess of the metal ions. Concentrations of the ligands were 2.0×10^{-3}−3.5×10^{-3} M and those of the metal ions 0.1 (Na^+, Tl^+, Ag^+) and 7.3×10^{-2} M (K^+). The initial solution volumes were 20.0 mL. The reliability of the equipment was tested by determining the thermodynamic quantities in absolute MeOH for Na^+−18-crown-6 interaction. Log *K* and ΔH values determined in our laboratory were in good agreement with the literature values.[1,2] The titration experiments showed that all interactions studied had a 1:1 cation/ligand ratio. Thermodynamic quantities for Ag^+ interactions exhibiting log *K* values larger than 5.5 were determined by a cation competition (with $NaNO_3$) technique.[21] In the cases of **2**−**6**, however, log *K* values for Ag^+ complexation were still too large to be determined accurately (Table 3). The ΔH values for these interactions were also evaluated from a direct titration. The results showed that the ΔH values obtained by direct and competitive titrations were in good agreement. The method used to process the calorimetric data and to calculate the log *K* and ΔH values has been described.[22]

Determination of Protonation Constants. The protonation constants of **2**−**7** were determined by potentiometric titration in MeOH at 25 °C. The titrations were carried out at a constant ionic strength of 0.10 M $(CH_3)_4NCl$ using an automatic microprocessor-controlled potentiometric titrator.[23] A 4.0×10^{-2} M ligand solution (5.0 mL) containing 0.12 M HCl was titrated by a 0.18 M Me_4NOH solution. Potentials to within ±0.1 mV were measured by using an Orion Model 701A digital ion analyzer in conjunction with an Orion combination electrode. The initial potentials were larger than 600 mV, and 60−100 intermittent titrations (0.020 mL each) brought the potentials to less than −100 mV. The new electrode was conditioned in 2 M $(CH_3)_4NCl$ solutions stepwise to 100% MeOH over a 10-day period, starting with the 2 M salt in 90% H_2O−10% MeOH solution. The MeOH was increased by 10% per day while the H_2O was decreased by 10%. Temperature was controlled within ±0.1 °C by using a jacketed cell through which water from a constant-temperature bath was circulated. Calculations were performed with the SUPERQUAD program[24] using an IBM computer.

^{1}H NMR and UV−Visible Spectral Measurements. ^{1}H NMR spectra of free and complexed ligands were recorded using a Varian Gemini 200 (200 MHz) spectrometer at 25.0 ± 0.1 °C in deuterated dimethyl sulfoxide (DMSO-d_6). Tetramethylsilane (TMS) was used as the internal standard. The DMSO-d_6 was used since the OH proton signals could be observed in this solvent.[25,26] The DMSO-d_6 solvent was treated with 3A molecular sieves in order to remove traces of water. The water content was monitored by taking the solvent ^{1}H NMR spectrum until the water peak was negligible. All OH peaks for free and complexed macrocycles detected by the ^{1}H NMR technique were confirmed by D_2O exchange reactions.[26,27]

UV−visible spectra were recorded at 23 ± 1 °C in a 1-cm quartz cell by using a Hewlett-Packard 8452A diode array spectrophotometer.

(16) Bordunov, A. V.; Hellier, P. C.; Bradshaw, J. S.; Dalley, N. K.; Kou, X.-L.; Zhang, X. X.; Izatt, R. M. *J. Org. Chem.* **1995**, *60*, 6097.
(17) Gokel, G. W.; Trafton, J. E. In *Cation Binding by Macrocycles*; Inoue, Y., Gokel, G. W., Eds.; Marcel Dekker: New York, 1990; Chapter 6.
(18) Arnold, K. A.; Hernandez, J. C.; Li, C.; Mallen, J. V.; Nakano, A.; Schall, O. F.; Trafton, J. E.; Tsesarskaja, M.; White, B. D.; Gokel, G. W. *Supramol. Chem.* **1995**, *5*, 45.
(19) Izatt, R. M.; Zhang, X. X.; An, H. Y.; Zhu, C. Y.; Bradshaw, J. S. *Inorg. Chem.* **1994**, *33*, 1007.
(20) (a) Oscarson, J. L.; Izatt, R. M. In *Physical Methods of Chemistry. Vol. VI: Determination of Thermodynamic Properties*; Rossiter, B. W., Baetzold, R. C., Eds.; John Wiley & Sons: New York, 1992; Chapter 7. (b) Izatt, R. M.; Wu, G. *Thermochim. Acta* **1989**, *154*, 161. (c) Eatough, D. J.; Izatt, R. M.; Christensen, J. J. In *Biochemical and Clinical Application of Thermometric and Thermal Analysis*; Jesperson, N., Ed.; Elsevier: New York, 1982; Chapters 2 and 7.
(21) Lamb, J. D.; Izatt, R. M.; Swain, C. S.; Christensen, J. J. *J. Am. Chem. Soc.* **1980**, *102*, 475.
(22) (a) Eatough, D. J.; Christensen, J. J.; Izatt, R. M. *Thermochim. Acta* **1972**, *3*, 219. (b) Eatough, D. J.; Izatt, R. M.; Christensen, J. J . *Thermochim. Acta* **1972**, *3*, 233.
(23) Gampp, H.; Maeder, M.; Zuberbühler, A. D.; Kaden, T. A. *Talanta* **1980**, *27*, 513.
(24) Gans, P.; Sabatini, A.; Vacca, A. *J. Chem. Soc., Dalton Trans.* **1985**, 1195.
(25) Chapman, O. L.; King, R. W. *J. Am. Chem. Soc.* **1964**, *86*, 1256.
(26) Silverstein, R. M.; Bassler, G. C.; Morrill, T. C. *Spectrometric Identification of Organic Compounds*, 5th ed.; John Wiley & Sons: New York, 1991; Chapter 4 (Proton NMR) and Chapter 7 (UV Spectrometry).
(27) McMurry, J. *Organic Chemistry*; Brooks/Cole Publishing: Pacific Grove, CA, 1988; p 948.

Table 1. Crystallographic Data and Refinement Details for $Na^+-\mathbf{3}$[a]

formula: $[Na(C_{23}H_{28.5}N_3O_5)]0.5\ ClO_4$	
fw = 499.7	$Z = 2$
space group: $P\bar{1}$ (No. 2)	temp = 20 °C
$a = 9.400(9)$ Å	$\mu = 1.59\ cm^{-1}$
$b = 11.467(10)$ Å	$F(000) = 526$
$c = 12.281(11)$ Å	$\lambda = 0.710\ 73$
$\alpha = 77.22(7)°$	no. of reflections measured: 3635
$\beta = 87.73(7)°$	no. of reflections with $F > 4\sigma(F)$: 1836
$\gamma = 86.39(7)°$	data/parameter: 5.9:1
$V = 1288(2)$ Å^3	$R^b = 8.27\%$
$\rho(calc) = 1.288\ g/cm^3$	$R_w{}^b = 9.27\%$ (unit weights)

[a] Uncertainties in the last significant digits are shown in parentheses. [b] $R = \sum||F_o| - |F_c||/\sum|F_o|$, $R_w = [\sum_w(|F_o| - |F_c|)^2/\sum_w(F_o)^2]^{1/2}$.

Absolute MeOH was used as the solvent. Concentrations were $10^{-4}-10^{-5}$ M for the ligands and 40 times the ligand concentrations for the metal ions.

Preparation of the Crystalline Complex. An attempt was made to prepare the $AgClO_4-\mathbf{3}$ complex as follows. A mixture of 0.066 g (0.63 mmol) of triethylamine and 0.27 g (0.63 mmol) of **3** in 10 mL of ethanol was refluxed for a few minutes. A solution of 0.13 g (0.63 mmol) of $AgClO_4 \cdot H_2O$ in 10 mL of ethanol was added dropwise to the above hot solution. A white precipitate immediately formed. The mixture was refluxed for 15 min and filtered hot. The hot solid turned black. (*Caution*! Perchlorate salts of metal complexes with organic ligands are potentially explosive. They must be handled very carefully and in small quantities). The filtrate was allowed to stand at room temperature whereupon some clear crystals separated. The crystals were filtered, air-dried, and carefully recrystallized from ethanol. These recrystallized crystals were shown by the following X-ray structural analysis to contain Na^+ rather than Ag^+ ion. An FAB MS analysis exhibited fragments at *m*/*e* 319.2 $(NaC_{15}H_{24}N_2O_4)^+$, which is (Na−azapyridino-18-crown-6)$^+$, 450.2 $(NaC_{23}H_{29}N_3O_5)^+$ which is (Na−**3**)$^+$, and 899.4 $(Na_2C_{46}H_{57}N_6O_{10})^+$ which is $(Na_2-\mathbf{3}_2 - H)^+$.

X-ray Structure Determination. A plate-shaped crystal prepared above with approximate dimensions of 0.1 × 0.2 x 0.3 mm was selected for the structural study. Crystal and intensity data were obtained using a Siemens R3m/V automated diffractometer which used graphite-monochromated Mo Kα radiation ($\lambda = 0.710\ 73$ Å). The orientation matrix and lattice parameters of the crystal were obtained using a least-squares procedure involving 30 ($6.99° < 2\theta < 30.05°$) carefully centered reflections. Intensities were measured using a variable scan rate $2\theta-\theta$ procedure with the scan speed determined by the intensities of the reflections. Data were collected to a 2θ limit of 45.0° with the index limits $-10 \le h \le 10$, $-12 \le k \le 12$, $0 \le l \le 13$. A total of 3635 reflections (3388, independent data $R_{int} = 1.61\%$) were collected. Of these data, 1836 ($F > 4\sigma(F)$) were used in the final refinement. Three standard reflections measured every 97 reflections showed no significant systematic changes. Crystallographic data, listed in Table 1, established that the complex crystallized in the triclinic crystal system and the intensity statistics ($E^2 - 1 = 0.978$) indicated that the proper space group for the crystal was $P\bar{1}$. This choice of space group was supported by the successful solution of the structure. An attempt was made to refine the structure in the noncentrosymmetric space group *P*1. While the final *R* value was below 15%, the large correlation coefficients between parameters of atoms that would be related by the presence of an inversion center verified that $P\bar{1}$ was the proper space group. Unit weights were applied to the data set which was not corrected for absorption or extinction effects.

The crystal structure was solved using direct methods, as positions for all non-hydrogen atoms were apparent in the *E* map. Initial refinement using only non-hydrogen atoms indicated severe disorder of the perchlorate ion. The disorder was resolved, using difference maps, into two orientations for the perchlorate oxygen atoms. The occupancy factors of the two sets of oxygen atoms were assigned the same value. Both perchlorate ion orientations were refined as rigid bodies with the Cl−O distances set at 1.40 Å. Positions for all hydrogen atoms bonded to carbon atoms were calculated with the C−H bond distances set at 0.96 Å. These hydrogen atoms were assigned isotropic displacement coefficients which were not refined. After anisotropic refinement of all non-hydrogen atoms except the oxygens of the disordered perchlorate ion, it was possible to find the position of the phenol hydrogen atom, H29, in a difference map. The relatively large final *R* value of 8.27% is due to the disorder of the perchlorate ion. The seven largest peaks in the difference map were near the chlorine atom, which indicated that the model proposed to describe the disorder was not quite right. The largest peak and hole in the difference map were 0.66 e Å^{-3} and 0.42 e Å^{-3}, respectively. Atomic scattering factors were obtained from the literature.[28] All programs used in the solution, refinement, and display of the $Na^+-\mathbf{3}$ complex were included in the SHELXTL-PLUS (VMS) program package.[29]

Table 2. Log *K* Values[a] for Protonation of the Macrocyclic Ligands in Methanol at 25.0 °C and $\mu = 0.10$ ($(CH_3)_4NCl$)

ligand	log K_1	log K_2	log K_3	$\sigma_p{}^b$
2	12.36 ± 0.04	7.96 ± 0.06	3.81 ± 0.08	0.78
3	12.50 ± 0.02	8.16 ± 0.04	3.87 ± 0.04	0.66
4	12.93 ± 0.05	8.25 ± 0.06	3.75 ± 0.08	0.23
5	13.31 ± 0.03	8.86 ± 0.07	3.97 ± 0.05	−0.17
6	13.38 ± 0.03	8.90 ± 0.08	3.71 ± 0.07	−0.27
7	8.63 ± 0.02	7.90 ± 0.04	1.75 ± 0.05	

[a] $K_1 = [HL]/[L^-][H^+]$, $K_2 = [H_2L^+]/[HL][H^+]$, and $K_3 = [H_3L^{2+}]/[H_2L^+][H^+]$. The HL denotes the ligands **2**−**7** in Figure 1. Values are the averages taken from two to four determinations. Uncertainties are given as standard deviations. [b] Hammett substituent constants (σ_p) for *p*-substituted phenol groups are from Pine, S. H. *Organic Chemistry*, 5th ed.; McGraw-Hill: New York, 1987; p 634.

Results and Discussion

Protonation Constants and Effect of Para Substituents of Phenol Groups on Metal Complexation. Log *K* values for protonation of the macrocyclic compounds in MeOH at 25.0 °C are listed in Table 2. Compounds **2**−**7** have three protonation constants. In each case, the log K_1 value is attributed to protonation of the phenolate group ($K_1 = [HL]/[L^-][H^+]$, where HL denotes the ligands **2**−**7**).[30] Log K_2 and log K_3 values correspond to protonation of the macroring-pivot and pyridine nitrogens ($K_2 = [H_2L^+]/[HL][H^+]$ and $K_3 = [H_3L^{2+}]/[H_2L^+][H^+]$). The para substituents of the phenol groups of **2**−**6** play an important role in the phenolate basicity, as shown by the log K_1 values, which increase in the sequence **2** < **3** < **4** < **5** < **6**. This is also the sequence of the log *K* values for the formation of the metal ion complexes. A plot of log K_1 against the Hammett σ_p constants (Figure 2) shows a straight line, indicating that the Hammett correlation holds for the phenol groups attached to the azacrown ring.

The smaller log K_1 value for protonation of the phenol group of **7** is probably due to the presence of the vicinal macroring oxygen atoms. It has been observed that the macroring donor atoms decrease the protonation constant of bromophenol incorporated into the macrocyclic backbone.[31]

Thermodynamic quantities (log *K*, ΔH, $T\Delta S$) for interactions of **1**−**8** with metal cations in MeOH at 25.0 °C are listed in Table 3. Pendant phenol arms play an important role in cation binding. Ligand **1**, without a pendant arm, shows very weak interaction with Na^+. However, ligands **2**−**6** with different phenol arms complex Na^+ with log *K* values of 3.06−3.59. The shape and the binding sites of ligands **2**−**6** are the same, and only the para substituents of the phenol groups are different. This difference results in different cation-binding abilities by

(28) Ibers, J. A.; Hamilton, W. C., Eds. *International Tables for X-Ray Crystallography*; Kynoch Press: Birmingham, U.K., 1974; Vol. 4.
(29) Sheldrick, G. M. SHELXTL PLUS Version 4.2, Siemens Analytical Instruments, Madison, WI, 1990.
(30) Czech, A.; Czech, B. P.; Bartsch, R. A.; Chang, C. A.; Ochaya, V. O. *J. Org. Chem.* **1988**, *53*, 5.
(31) Kimura, E.; Kimura, Y.; Yatsunami, T.; Shionoya, M.; Koike, T. *J. Am. Chem. Soc.* **1987**, *109*, 6212.

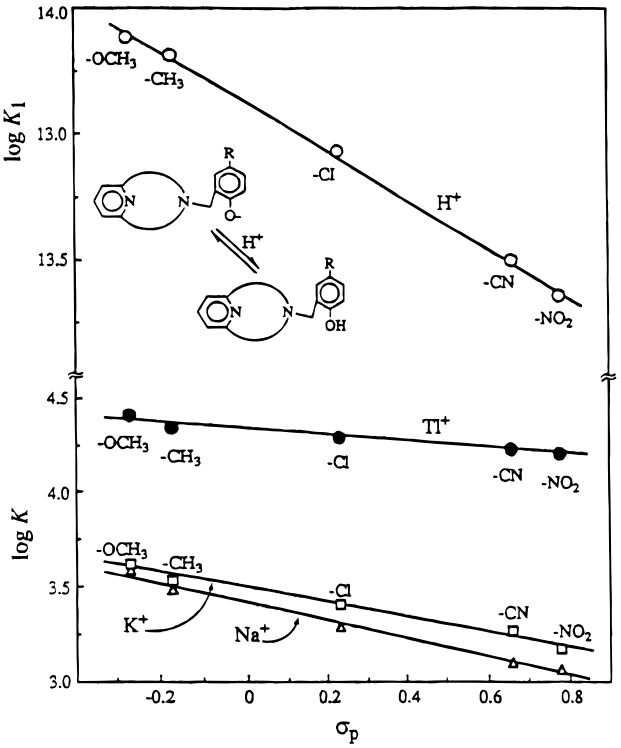

Figure 2. Hammett plots for protonation and metal ion complexation of macrocyclic compounds **2**−**6**.

the ligands. Log *K* values for complexation of Na^+, K^+, and Tl^+ with **2**−**6** have the same sequence, i.e., **2** < **3** < **4** < **5** < **6**. This sequence is consistent with the electron-donating ability of the phenol substituents (NO_2 < CN < Cl < CH_3 < OCH_3). Plots of log *K* values against the Hammett σ_p constants show a good linear relationship in each case (Figure 2). Smid and coworkers have observed a similar Hammett linear correlation for complexation of 4′-substituted benzo-15-crown-5 with Na^+ but not of 4′-substituted benzo-18-crown-6 with Na^+ and K^+.[32] In our cases, however, all three cations (Na^+, K^+, Tl^+) show the Hammett correlations.

The Hammett correlations for complexation of **2**−**6** with the cations can be understood as follows. The para substituents on the phenol groups result in a change in basicity of the phenolate group, as mentioned above, and in turn result in different stabilities of the complexes. Both enthalpy and entropy effects contribute to the change of the complex stabilities involving ligands **2**−**6**. In the cases of Na^+ and K^+, the increase in log *K* values from **2** to **4** is due to increased $-\Delta H$ values while that from **4** to **6** is due to decreased $-T\Delta S$ values (Table 3). A similar situation is observed for Tl^+. The increase in log *K* values from **2** to **5** is due to increased $-\Delta H$ values while that from **5** to **6** is a result of a decreased $-T\Delta S$ value.

Complexation Thermodynamics. As can be seen in Table 3, the phenol-substituted pyridinoazacrown ethers **2**−**6** form stable complexes with Na^+, K^+, Tl^+, and Ag^+ in MeOH and show high selectivity for Ag^+ over the other cations studied. In each case, the log *K* values for complex formation increase in the order $Na^+ < K^+ < Tl^+ \ll Ag^+$. Selectivity factors of Ag^+ over Na^+, K^+, and Tl^+ by **2**−**6** are larger than 4 orders of magnitude. Ligands **7** and **8** selectively bind Ag^+ over Na^+, K^+, and Tl^+ by more than or near to 2 orders of magnitude. The location and orientation of the two nitrogen atoms in ligands **2**−**6** provide an ideal coordination site for Ag^+, which prefers linear coordination and shows a high affinity for nitrogen atoms.

(32) Ungaro, R.; El Haj, B.; Smid, J. *J. Am. Chem. Soc*. **1976**, *98*, 5198.

Table 3. Log *K*, ΔH (kJ/mol), and $T\Delta S$ (kJ/mol) Values[a] for Interactions of Macrocyclic Ligands with Metal Ions in Methanol at 25.0°C

ligand	cation	log *K*	ΔH	$T\Delta S$
1	Na^+	*b*		
	Ag^+	>5.5	−39.4 ± 0.8	>−8.0
2	Na^+	3.06 ± 0.03[c]	−20.8 ± 0.5	−3.3
	K^+	3.17 ± 0.04[c]	−32.9 ± 0.4	−14.8
	Tl^+	4.20 ± 0.02	−26.2 ± 0.4	−2.2
	Ag^+	>8.5[c,d]	−59.0 ± 0.5[d]	>−10.5
3	Na^+	3.10 ± 0.04	−22.2 ± 0.7	−4.5
	K^+	3.27 ± 0.03	−37.2 ± 0.2	−18.5
	Tl^+	4.22 ± 0.03	−31.9 ± 0.5	−7.8
	Ag^+	>9[d]	−59.4 ± 0.5[d]	>−8.0
4	Na^+	3.29 ± 0.04[c]	−23.3 ± 0.6	−4.5
	K^+	3.41 ± 0.05	−38.4 ± 0.3	−18.9
	Tl^+	4.29 ± 0.03	−37.9 ± 0.4	−13.4
	Ag^+	>9[d]	−59.8 ± 0.5[d]	>−8.4
5	Na^+	3.49 ± 0.05[c]	−23.1 ± 0.6	−3.2
	K^+	3.53 ± 0.02	−37.7 ± 0.3	−17.6
	Tl^+	4.34 ± 0.02	−39.5 ± 0.2	−14.7
	Ag^+	>9[d]	−63.6 ± 0.8[d]	>−12.2
6	Na^+	3.59 ± 0.04[c]	−21.8 ± 0.5	−1.3
	K^+	3.62 ± 0.03[c]	−33.8 ± 0.4	−13.1
	Tl^+	4.40 ± 0.02	−38.9 ± 0.3	−13.8
	Ag^+	>9[d]	−61.2 ± 0.3[d]	>−9.8
7	Na^+	2.75 ± 0.05	−18.6 ± 0.8	−2.9
	K^+	3.00 ± 0.04	−27.8 ± 0.3	−10.7
	Tl^+	4.45 ± 0.04	−38.7 ± 0.6	−13.3
	Ag^+	6.33 ± 0.07[d]	−49.3 ± 0.6[d]	−13.2
8	Na^+	2.89 ± 0.06	−14.3 ± 0.7	2.2
	K^+	3.34 ± 0.03	−26.1 ± 0.5	−7.0
	Tl^+	4.76 ± 0.07	−35.8 ± 0.7	−8.6
	Ag^+	6.83 ± 0.06[d]	−41.6 ± 0.8[d]	−2.6

[a] Values are the averages taken from two to four determinations. Uncertainties are given as standard deviations. Ionic strength was not controlled, since there was no significant effect of ionic strength on the thermodynamic quantities under the conditions studied (see ref 19). [b] No measurable heat other than heat of dilution indicating that ΔH or/and log *K* is small. [c] Reference 16. [d] Quantities were determined by competitive calorimetric titration.

The $-\Delta H$ values for interactions of **2**−**6** with Ag^+ are significantly higher than those with Na^+, K^+, and Tl^+, which is attributed to the stronger affinity of Ag^+ for the nitrogen atoms. In addition, the oxygen donor atoms in the macroring and the phenol arm participate in the bonding and shelter the cation from the solvation. Therefore, the phenol-substituted pyridinoaza-18-crown-6 ligands (**2**−**6**) show excellent Ag^+-binding ability.

In a previous study,[9] it was shown that pyridonothia-18-crown-6 selectively bound Ag^+ over Hg^{2+}, which was a reversal of the common Hg^{2+} over Ag^+ selectivity order demonstrated by most macrocyclic ligands. ^{13}C NMR data indicated that Ag^+ interacted strongly but Hg^{2+} weakly with the pyridone nitrogen. This difference in cation affinities played a key role in the Ag^+ selectivity. The linear coordination of the pyridone nitrogen and macroring sulfur atoms with Ag^+ brought the cation into the macrocycle cavity making cation−dipole interaction with the ether oxygen atoms possible. Similarly, the linear N−Ag^+−N coordination in **2**−**6** complexes results in a high Ag^+ selectivity. All donor atoms of the ligands **2**−**6** are capable of interacting with the cation providing a direct coordination sphere, as shown by ^1H NMR and X-ray crystallographic data (see below). Thus, pyridine-containing 18-crown-6 ligands, together with a linear coordination site provided by two high-Ag^+-affinity atoms (nitrogen or sulfur), usually result in high Ag^+ selectivity.

Ligands **7** and **8** display much lower Ag^+ selectivity than **2**−**6**, indicating that the pyridine moiety incorporated into the macroring (**2**−**6**) plays a more important role in Ag^+ binding than does the pendant pyridine group of **7** and **8**. The location

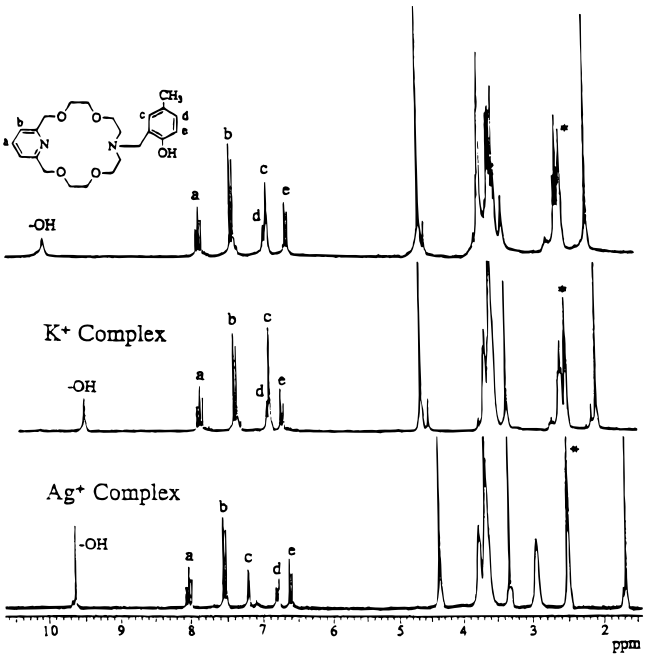

Figure 3. ^{1}H NMR spectra of free **5** and its K^+ and Ag^+ complexes in DMSO-d_6. Peak assignments are shown for aromatic and OH protons. The peaks labeled with an asterisk are attributed to the solvent.

of the two nitrogen atoms in **7** and **8** leads to a loss of the linear coordination of the nitrogen atoms with Ag^+. This is probably the main reason for decreased Ag^+ selectivity. The $-\Delta H$ values for Ag^+ interaction with **7** and **8** are significantly smaller than those with **2**−**6** (Table 3), indicating that the affinity of Ag^+ with the nitrogen atoms of **7** and **8** is much weaker than that with those of **2**−**6**.

In each case, the higher stability of the complexes of the metal ions with **8** than with **7** suggests that the methoxy group is more favorable for the cation binding than the hydroxyl group. Since the ΔH values for **8**−M^+ interactions are less negative while the $T\Delta S$ values are more favorable (in the case of Na^+) or less unfavorable than those for **7**−M^+ interactions (Table 3), the more stable complexes of **8** originate from the entropic contributions. The same effect was observed previously.[19,33]

Ligand **7** is an isomer of **5**, but it shows different complexation behavior. Compound **7** forms less stable complexes than **5** with Na^+, K^+, and Ag^+. The Tl^+ complexes of the two ligands have similar log *K*, ΔH, and $T\Delta S$ values, probably due to the large Tl^+ size which results in a similar spherical coordination. The more favorable ΔH and less unfavorable $T\Delta S$ values for **5**−Ag^+ complexation (−63.6 and > −12.2 kJ/mol, respectively) than those for **7**−Ag^+ complexation (−49.3 and −13.2 kJ/mol, respectively) suggest a linear N−Ag^+−N coordination geometry in the **5**−Ag^+ but not in the **7**−Ag^+ complex.

^{1}H NMR Spectra. ^{1}H NMR spectra of free and complexed **2** and **5** are shown in Figures S1 (all figures designated with an "S" are found in Supporting Information) and 3. Chemical shifts of aromatic and hydroxyl protons of free and complexed ligands **1**−**7** are listed in Table 4. Upon complexation with the metal ions, all proton signals of the ligands undergo chemical shift changes of varying magnitudes indicating the interactions of the cations with both macroring and pendant arms. It is seen in Figure 3 that the spectra of the complexed ligand are different from that of the free one. More significant changes in the ^{1}H NMR spectra are produced by the strong interaction of Ag^+ than by the weak interaction of K^+ with the same ligands (Table 4).

Table 4. Chemical Shifts (δ in ppm)[a] of Aromatic and Hydroxyl Protons of Free and Complexed Pyridinoazacrown Ethers and Cation-Induced Shifts (CIS)[b] in DMSO at 25.0 °C

compd	H_a	H_b	H_c	H_d	H_e	H_{OH}
1	7.776	7.312				
1−Ag^+	8.061	7.606				
	(−57.0)	(−58.8)				
2	7.785	7.328	8.052	7.987	6.800	no
2−Na^+	7.814	7.315	8.140	8.027	6.849	no
	(−5.80)	(2.60)	(−17.6)	(−8.00)	(−9.80)	
2−K^+	7.814	7.328	8.068	8.012	6.929	no
	(−5.80)	(0)	(−3.20)	(−5.00)	(−25.8)	
2−Tl^+	*c*	7.341	*c*	*c*	6.106	no
		(−2.60)			(139)	
2−Ag^+	7.960	7.485	8.383	7.998	6.927	no
	(−35.0)	(−31.2)	(−66.2)	(−2.20)	(−25.4)	
3	7.787	7.327	7.553	7.507	6.802	no
3−Na^+	7.814	7.313	7.684	7.551	6.872	no
	(−5.40)	(2.80)	(−26.2)	(−8.80)	(−14.0)	
3−K^+	7.812	7.326	7.608	7.543	6.921	no
	(−5.00)	(0.20)	(−11.0)	(−7.20)	(−23.8)	
3−Tl^+	7.800	7.348	7.190	7.230	6.297	no
	(−2.60)	(−4.20)	(72.6)	(55.4)	(101)	
3−Ag^+	8.017	7.526	7.937	7.470	6.856	11.18
	(−46.0)	(−39.8)	(−76.8)	(7.40)	(−10.8)	
4	7.785	7.325	7.130	7.068	6.678	3.310[d]
4−Na^+	7.796	7.320	7.160	7.101	6.697	10.35[d]
	(−2.20)	(1.00)	(−6.00)	(−6.60)	(−3.80)	
4−K^+	7.811	7.326	7.149	7.099	6.790	10.00[d]
	(−5.20)	(−0.20)	(−3.80)	(−6.20)	(−22.4)	
4−Ag^+	8.012	7.519	7.509	7.056	6.739	10.22
	(−45.4)	(−38.8)	(−75.8)	(2.40)	(−12.2)	
5	7.787	7.325	6.831	6.856	6.549	10.01[d]
5−K^+	7.819	7.331	6.854	6.866	6.678	9.460
	(−6.40)	(−1.20)	(−4.60)	(−2.00)	(−25.8)	
5−Ag^+	8.021	7.531	7.213	6.796	6.607	9.631
	(−46.8)	(−41.2)	(−76.4)	(12.0)	(−11.6)	
6	7.787	7.325	6.603	6.610	6.635	9.704[d]
6−K^+	7.817	7.327	*c*	*c*	*c*	9.222[d]
	(−6.00)	(−0.40)				
6−Ag^+	8.013	7.513	6.609	6.989	6.594	9.429
	(−45.2)	(−37.6)	(−1.20)	(−75.8)	(8.20)	
7	6.947	8.448	7.216	7.693	7.447	7.999
7−Ag^+	7.058	8.120	7.402	7.903	7.441	8.855
	(−22.2)	(65.6)	(−37.2)	(−42.0)	(1.20)	

[a] Concentrations of the ligands were ~0.01 M and those of the metal ions were 0.05−0.08 M. The chemical shifts are referred to internal Me_4Si. [b] CIS (Hz) = 200[δ_{lig} (ppm) − δ_{compl} (ppm)]. The CIS values (Hz) are in parentheses. A negative value indicates a downfield shift while a positive value an upfield shift. [c] The peak shape has a large change as compared to that of the free ligand. [d] The peak is broad.

The cation-induced shift (CIS) values for aromatic and hydroxy protons are informative. Upon complexation with the metal ions, most aromatic protons display downfield shifts (Table 4, negative CIS values in parentheses), indicating that both pyridine and phenol groups interact with the cations. In the cases of **2**−**6**, Ag^+ causes much larger downfield shifts for pyridine protons (H_a, H_b) than do the Na^+, K^+, and Tl^+, suggesting a strong interaction between Ag^+ and the pyridine nitrogen atom. This observation is in accordance with the relative magnitudes of the binding constants for these cations in MeOH (Table 3). The Ag^+ also induces large downfield shifts for pyridine protons of ligand **1** due to the expected strong interaction (log *K*(MeOH) > 5.5). Strong interaction between Ag^+ and the pyridine moiety of the macrocyclic ligands can also be seen from the large proton signal shifts of the methylene groups adjacent to the pyridine group. These protons show strong single peaks at 4.58 ppm in the free ligands, and the peaks are shifted to 4.41 and 4.37 ppm in the Ag^+−**2** and Ag^+−**5** complexes, respectively (Figures S1 and 3). On the

(33) Arnold, K. A.; Echegoyen, L.; Fronczek, F. R.; Gandour, R. D.; Gatto, V. J.; White, B. D.; Gokel, G. W. *J. Am. Chem. Soc.* **1987**, *109*, 3716.

Table 5. UV−Visible Absorbance Peaks (λ_{max}) and Molar Absorptivity (ϵ) Values[a] for Macrocycles **2**−**4** and **6** in Methanol

species	λ_{max} (ϵ/10^3)			
2	231 (7.18)	264 (5.20)	269 (4.93)	324 (8.10)
2−Na^+	230 (10.8)	264 (7.78)	270 (7.57)	313 (11.4)
2−$Na^+(OH^-)$[e]		264 (8.00)	271,sh(6.78)	407 (21.6)
3		254 (18.7)	269,sh (9.64)	
3−Na^+		251 (18.7)	270,sh (8.07)	
3−K^+		250 (20.5)	270,sh (8.68)	
3−Tl^+	*b*	280 (18.4)		
3−Ag^+	*b*	272 (20.4)		
3−$Na^+(OH^-)$[e]		281 (22.6)		
4	231 (9.06)	264 (4.34)	269 (3.97)	286 (2.43)
4(H^+)[e]	228 (10.3)	*d*	271 (9.90)[d]	*d*
4(OH^-)[e]	232 (9.26)	250 (6.00)	265, sh (5.37)	291 (2.68)
4−Na^+	228 (9.30)	264 (4.79)	270 (4.34)	283 (2.19)
4−Tl^+	*b*	*b*	*b*	285 (2.64)
4−$Na^+(OH^-)$[e]	*d*	251 (13.8)[d]	*d*	307 (4.10)
6	228 (7.18)	264 (3.91)	269 (3.44)	295 (3.49)
6−K^+	226,sh (7.54)	264 (4.17)	271 (3.78)	294 (3.62)
6−Tl^+	*b*	*b*	*b*	296 (3.56)
6−Ag^+	*b*	266 (4.34)[d]	*d*	300 (3.86)

[a] λ_{max} and ϵ values are in nm and M^{-1} cm^{-1}, respectively. All ϵ values have been multiplied by 10^{-3}. sh = shoulder. [b] Extremely strong absorption caused by $Tl(CH_3CO_2)$ (λ_{max} = 219 nm, $\epsilon = 5.85 \times 10^3$ M^{-1} cm^{-1}) or $AgNO_3$ (λ_{max} = 205 nm, $\epsilon = 1.05 \times 10^4$ M^{-1} cm^{-1}). [c] No absorption observed. [d] The peaks were merged. [e] In 0.010 M HCl (H^+) or 0.010 M $(CH_3)_4NOH$ (OH^-) MeOH sulotion.

other hand, the shifts of these peaks in the K^+−**2** and K^+−**5** complexes are much smaller (both to 4.62 ppm). Significant chemical shifts induced by Ag^+ for phenol-ring protons (H_c, H_d, or H_e; see Table 4) of **2**−**6** suggest that the phenol arms also bind Ag^+.

All free and complexed ligands of **4**−**7** show OH proton signals (Figure 3, Table 4). This observation demonstrates that ligands **4**−**7** form complexes with the cations in their phenol forms and the complexation does not deprotonate the ligands. The same effect has been observed for other phenol-containing macrocycles.[34] In most cases involving **2** and **3**, on the other hand, no OH signal can be detected (Table 4). This observation does not imply that **2** and **3** and their complexes exist as phenolate forms in MeOH. The UV−visible data reveal that in MeOH the phenol protons are not ionized from the ligands (see below). An X-ray crystal structure of **2** shows that the phenol group of the ligand is not deprotonated.[16] Compared with **4**−**6**, the greater acidity of the phenol groups of **2** and **3** could result in a fast kinetic exchange of the OH protons so that the signals would be greatly broadened and be difficult to detect.

For the free macrocyclic ligands **2**−**6**, ^1H NMR peak positions of the pyridine protons are fixed (averages of H_a and H_b are 7.786 and 7.326 ppm, respectively, both with a ±0.001 ppm deviation) while those of phenol-ring protons (H_c−H_e) change with different substituents. With increasing electron-donating ability of the substituents (NO_2 < CN < Cl < CH_3 < OCH_3), the H_c, H_d, and H_e signals shift to higher field (lower δ values). This observation is not surprising since the electron-donating substituents increase electron density of the aromatic ring and increase the magnetic shielding effect.

UV−Visible Spectra. UV−visible spectral data (above 220 nm) valid in MeOH are listed in Table 5. Spectra of free and complexed ligands **2** and **4** are shown in Figures 4 and S2. Above 220 nm (below 220 nm the metal salts show strong

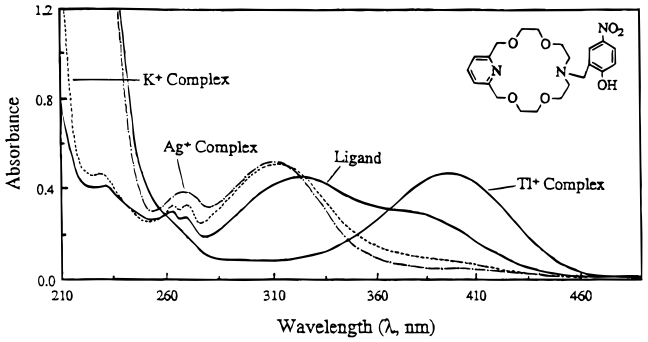

Figure 4. UV−visible spectra of free and complexed **2** in MeOH. [**2**] = 6.63×10^{-5} M for K^+ (2.57×10^{-3} M) and Ag^+ (2.44×10^{-3} M) and 3.31×10^{-5} M for Tl^+ (1.28×10^{-3} M).

absorption), the phenol-substituted pyridinoazacrown ethers (except **3**) exhibit four absorption bands which originate from aromatic ring substituents (phenol and pyridine). Absorption peaks in the vicinity of 230 (K band) and 290 nm (B band, 324 nm for **2**) are from phenol and those in the vicinity of 260 and 270 nm (B band) from pyridine.[26,34] Upon complexation with the metal ions, changes in absorption maxima or/and in peak intensities of the ligands are observed, indicating the interactions of both phenol and pyridine groups with the cations. Ag^+ results in merging of the two pyridine absorption peaks while K^+ and Na^+ exhibit no such effect (Figures 4 and S2 and Table 5). This difference is probably a result of the stronger interaction of the pyridine nitrogen atom of the ligands with Ag^+ than with K^+ and Na^+, which is in accordance with the thermodynamic and ^1H NMR data. In neutral MeOH, both absorption maxima and intensities of the phenol groups of the **4** and **6** complexes do not change very greatly from those of the free ligands, suggesting that the complexation does not deprotonate these phenol groups. These results are also consistent with those obtained from ^1H NMR spectral data.

UV−visible data indicate that the phenol groups of **2** and **3** are not completely ionized. Because of higher acidity and larger π area of the *p*-nitrophenol group, ligand **2** and its complexes show significantly different UV−visible spectra from **4** and **6**. As compared with **4** and **6**, a large bathochromic shift of the B band (to 324 nm, Figure 4) of the phenol absorption is observed for free **2** and absorption intensity is increased greatly (Table 5). With such an absorption band, we doubted the deprotonation of the phenol group of **2**. However, the UV−visible spectrum of **2** in an alkaline medium (0.010 M Me_4NOH) shows a further large bathochromic shift of the B band to 408 nm and a further intensification (Figure S3), indicating that in the neutral MeOH solution the phenol OH is not deprotonated. We have also found the UV−visible spectrum of **2** in an acidic MeOH medium (0.010 M HCl) to be different from that in a neutral MeOH solution (Figure S3). The peak at 324 nm in the neutral solution shifts to 303 nm, and the yellow color of the solution disappears in the acidic solution. These facts suggest that in the neutral MeOH solution the phenol group of **2** is neither deprotonated nor a normal O−H bond.

It has been conclusively demonstrated that formation of the hydrogen bond results in a red shift and in the intensification of the B (^1L_b) band of phenol and that this effect weakens the phenol O−H bond.[35] Therefore, a possible state of the phenol group of **2** in neutral MeOH solution is that the phenol OH forms a hydrogen bond with a nitrogen atom of the ligand and the O−H bond is therefore weakened. The UV−visible spectra

(34) Zhang, X. X.; Bordunov, A. V.; Bradshaw, J. S.; Dalley, N. K.; Kou, X.-L.; Izatt, R. M. *J. Am. Chem. Soc.* **1995**, *117*, 11507.

(35) Mataga, N.; Kubota, T. *Molecular Interactions and Electronic Spectra*, Marcel Dekker: New York, 1970; pp 333−337.

agree with this point. In the acidic solution, protonation of the macroring nitrogen atoms breaks the hydrogen bond. Thus, the phenol group resumes its normal OH bond and the B band shifts to a shorter wavelength. In the alkaline solution, on the other hand, complete deprotonation of the phenol group results in a phenolate ion which absorbs UV−visible light at a longer wavelength with increased intensity. The crystal structure of **2** supports this point. In solid state, the phenol hydrogen forms an intramolecular hydrogen bond with the pivot nitrogen atom of the crown ring.[16]

The changes in the UV absorption spectra of **3** (Figure S4) with the acidity/basicity of the medium are similar to those of **2** (Figure S3), indicating that the phenol OH group of **3** is not deprotonated but forms a hydrogen bond with a donor atom of the ligand in neutral MeOH solution. Possible acid−base equilibria for the phenol-substituted macrocycles can be depicted as follows:

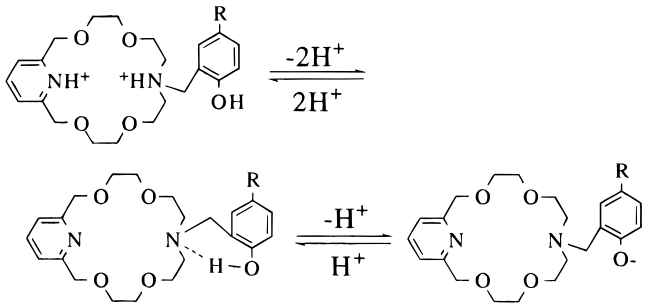

The UV spectrum of **3** is different from those of other phenol-substituted ligands (**2**, **4**−**6**). Above 220 nm, **3** shows only one strong absorption at 254 nm, which originates from $\pi-\pi^*$ transition of the cyanophenol.[26,36] The UV spectrum of 4-cyanophenol (pendant arm of **3**) in neutral MeOH solution measured in our laboratory is consistent with that in the literature.[36] The strong absorption of the cyanophenol of **3** overlaps absorption of the pyridine group, which shows only a shoulder peak at 269 nm (Figure S4).

A strong absorption of the Tl^+−**2** complex at 393 nm (Figure 4) suggests deprotonation of the ligand under this condition. The OH signal in the Tl^+−**2** complex was not observed in the ^{1}H NMR spectrum (Table 4).

Macrocycle **4** shows a slightly different spectral behavior from **2** and **3** due to the relatively lower acidity of the phenol group. It is not surprising to observe a hypsochromic shift of the B band of the phenol of **4** in 0.01 M HCl MeOH solution (to 271 nm, the band merges with the pyridine absorption) as compared with that in neutral MeOH solution (286 nm, Table 5). In alkaline medium, on the other hand, the phenol B band of **4** experiences only a small bathochromic shift (to 291 nm) and small intensification, indicating that 0.01 M base (Me_4NOH) is not strong enough to completely remove the phenol hydrogen of **4**. However, a significant bathochromic shift of the B band to 307 nm and an increase in intensity in the presence of both Na^+ and 0.01 M base suggest that the phenol hydrogen of **4** is ionized under this condition, which is probably a result of the coordination of the cation that weakens the O−H bond.

X-ray Crystal Structure. Each Na^+−**3** complex interacts with a symmetry related complex to form a dimer as shown in Figure 5. The phenol hydrogen atom, H29, plays an important role in the formation of the dimer. The position for H29 was found in a difference map and refined to a position 1.02 Å from O29, and in the final stages of the refinement the hydrogen atom was allowed to ride on O29. H29 forms a hydrogen bond with O29a (H29···O29a, 1.56 Å; O29−O29a, 2.489 Å; and the O29−H29···O29a angle, 148°). The presence of the center of symmetry in the structure suggests that a pair of hydrogen bonds links O29 to O29a as shown in Figure 5. However, this is not possible, as the interatomic distance between the H29 and H29a is too short (0.87 Å). In order to satisfy the symmetry requirements but have only one hydrogen bond linking the two complexes, the structure must consist of a statistically disordered arrangement in which a hydrogen atom is bonded to O29 in half the dimers and to O29a in the other half. This time-averaged structure is consistent with the center of inversion. Because one phenol in each dimer is ionized, the structure consists of a complex cation containing two Na^+−**3** units and one ClO_4^-. Thus, there is half a ClO_4^- for each Na^+−**3** unit and the complex has a formula $[Na(C_{23}H_{28.5}N_3O_5)](ClO_4)_{0.5}$. The asymmetric unit of the structure consists of one Na^+−**3** unit and half a ClO_4^-. Crystallographically, this means that only one of the two ClO_4^- sites associated with the dimer is occupied. Another model for the structure is possible in which a hydrogen atom is bonded to each phenol oxygen atom with neither hydrogen atom being involved in a hydrogen bond. In this case there would be one ClO_4^- for each Na^+−**3** unit. Both models were refined to approximately the same *R* value. The statistically disordered model was selected as the correct structure because the disorder of the perchlorate ion was resolved in a more satisfactory manner using that model and because it was not possible to find any other position for H29 in the difference map that would be required by the second model. In addition, it seemed highly unlikely that the O29...O29a interatomic distance could be 2.489 Å without a hydrogen bond being present.

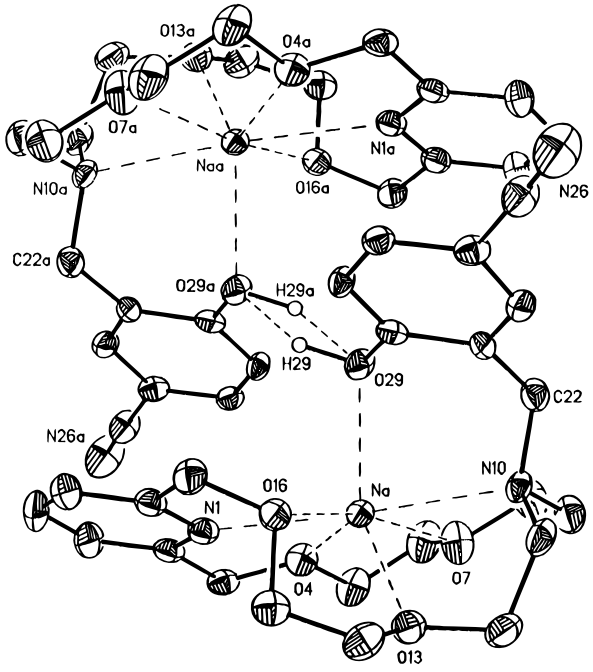

Figure 5. Crystal structure of the Na^+−**3** complex dimer. The thermal ellipsoids are drawn at the 25% probability level. The perchlorate ion and all hydrogen atoms except for H29 and H29a are omitted for clarity.

The Na^+ is coordinated by the seven donor atoms of the ligand. The geometry of the coordination polyhedron about the Na^+ is shown in Figure 5, and the Na^+...donor atom interatomic distances and donor atom−Na^+−donor atom angles are listed in Table 6. These data indicate that the coordination geometry

(36) (a) Phillips, J. P.; Bates, D.; Feuer, H.; Thyagarajan, B. S. *Organic Electronic Spectral Data*; John Wiley & Sons: New York, 1971; Vol. XIII, p 68. (b) Tsuzuki, Y.; Asabe, Y. *J. Chem. Eng. Data* **1971**, *16*, 108.

Table 6. Interatomic Distances and Angles for the Complex Na^+−**3**

1	2	3	1−2 (Å)	1−2−3 (deg)
N1	Na	O4	2.571(10)	62.2(3)
N1	Na	O7		125.7(3)
O4	Na	O7	2.518(8)	63.5(3)
N1	Na	N10		167.7(3)
O4	Na	N10		130.2(3)
O7	Na	N10	2.533(9)	66.6(3)
N1	Na	O13		105.0(3)
O4	Na	O13		117.7(3)
O7	Na	O13		98.3(3)
N10	Na	O13	2.635(9)	69.8(3)
N1	Na	O16		63.8(3)
O4	Na	O16		124.3(3)
O7	Na	O16		163.6(3)
N10	Na	O16		104.1(3)
O13	Na	O16	2.471(8)	65.3(2)
N1	Na	O29		96.4(3)
O4	Na	O29		116.9(3)
O7	Na	O29		108.9(3)
N10	Na	O29		78.7(3)
O29	Na	O13	2.400(8)	125.3(3)
O16	Na	O29	2.651(8)	81.3(3)

of Na^+ cannot be described in terms of a common coordination polyhedron. This is not unusual in the case of the coordination of an alkali metal cation. The shortest Na^+−donor atom distance involves the phenol oxygen atom (2.400 Å). The Na^+−macrocycle donor atom distances range from 2.471 to 2.651 Å. The coordination of the Na^+ can be described in three different ways: (1) a hexagonal pyramid with O29 as the apex atom, (2) a pentagonal bipyramid with N1 and N10 as the apex atoms, and (3) a pentagonal bipyramid with O7 and O16 as the apex atoms. Each proposed polyhedron is distorted.

As pointed out above, the hydrogen atom H29 links two Na^+−**3** molecules which are related by an inversion center. Interestingly, there is another intermolecular interaction between the two molecules that make up the dimer. The electron-deficient pyridine ring of one molecule and the electron-rich substituted phenol ring of the other are nearly parallel (Figure 5). The dihedral angle between the pairs of planar rings is 11.1°, and the distance between the centers of the rings is 3.75 Å. This relatively short interatomic distance and the presence of nearly parallel aromatic rings indicate the presence of $\pi-\pi$ interactions between the two molecules, which also contributes to the stability of the dimers. The $\pi-\pi$ interactions are enhanced by the presence of an ionized phenol and are additional evidence supporting the presence of the half perchlorate ion in the structure.

Conclusions

Seven new pyridine-containing macrocyclic ligands form stable complexes with Na^+, K^+, Tl^+, and Ag^+ in MeOH solution. In each case, log *K* values for the M^+−macrocycle interactions have the sequence $Na^+ < K^+ < Tl^+ \ll Ag^+$. The ligands having a pyridine unit incorporated into the macroring backbone and a phenol group attached as a pendant arm (**2**−**6**) selectively bind Ag^+ over the other cations by more than 4 orders of magnitude. Ligands **2**−**6** are more highly preorganized for Ag^+ binding than **7** and **8**, each of which has a pyridine unit attached as a pendant arm and a phenol or an anisole group incorporated into the macrocyclic backbone.

In the cases of **2**−**6**, the substituents on the para position of the phenol arm have an appreciable effect on phenol-protonation and cation-binding constants. Good Hammett correlations are found by plotting log *K* for interactions of five phenol-armed macrocyclic ligands (**2**−**6**) with H^+, Na^+, K^+, and Tl^+ vs σ_p.

Thermodynamic, spectroscopic, and X-ray crystallographic data indicate that in most cases the phenol-containing macrocycles exist as phenol forms in both free and complexed compounds. All donor atoms of the macroring and the pyridine and phenol arms of the ligands are able to interact with a cation, providing three-dimensional coordination. The phenol hydrogen is capable of forming either an intermolecular or an intramolecular hydrogen bond. Complexation with the metal ions studied in MeOH generally does not deprotonate the phenol group.

Acknowledgment. The authors thank the Department of Energy, Office of Basic Energy Sciences for financial support through Grant DE-FG02−86ER-13463. We appreciate valuable discussions with Dr. Alexander Y. Nazarenko concerning measurement of protonation constants.

Supporting Information Available: Tables listing crystal and experimental data, atomic positional, equivalent isotropic, and anisotropic thermal parameters, complete bond lengths and angles for non-hydrogen atoms, calculated H atom coordinates for the Na^+−**3** complex, and figures showing a thermal ellipsoid drawing of the Na^+−**3**, the dimer formed by two Na^+−**3** units, ^{1}H NMR spectra of free **2** and its K^+ and Ag^+ complexes, UV−visible spectra of free and complexed **4**, and UV−visible spectra of **2** and **3** in neutral, acidic, and basic MeOH solutions (11 pages). Ordering information is given on any current masthead page.

IC961263Q